

Effects of compatibilizer, compounding method, extrusion parameters, and nanofiller loading in clay-reinforced recycled HDPE/PET nanocomposites

Ruey Shan Chen, Sahrim Ahmad, Sinyee Gan, Mohd Hafizuddin Ab Ghani, Mohd Nazry Salleh

Material Science Programme, School of Applied Physics, Faculty of Science and Technology,
the National University of Malaysia, 43600 Bangi, Malaysia

Correspondence to: R. S. Chen (E-mail: rueyshanchen@hotmail.com)

ABSTRACT: Nanocomposites based on recycled high density polyethylene (rHDPE), recycled polyethylene terephthalate (rPET), and organoclay (C10A) were made using twin screw extruder followed by hot pressing. The independent effects of polymer/clay compatibility, preparation method, extrusion parameters, and clay loadings were investigated. Ethylene-glycidyl methacrylate could effectively improve the compatibilization of immiscible rHDPE/rPET blend with clay, which confirmed by the good polymers-clay adherence and domain size reduction obtained in scanning electron microscopy images. Although intercalated structures were observed in the composites made by one-step compounding, in the composites prepared by two-step extrusion method, enhanced dispersion of clay in polymer blend was found from X-ray diffraction results. Higher extrusion temperature and intermediate speed of rotation (90 rpm) appeared to increase the mechanical properties due to improvement of nanofiller dispersion in matrix. Results showed that the stiffness increased whereas tensile and impact strength decreased with clay content. © 2015 Wiley Periodicals, Inc. *J. Appl. Polym. Sci.* **2015**, *132*, 42287.

KEYWORDS: clay; composites; extrusion; properties and characterization; recycling

Received 16 December 2014; accepted 31 March 2015

DOI: 10.1002/app.42287

INTRODUCTION

The production and consumption of plastics globally account for notable contribution in municipal solid waste. Besides environmental concern, plastic wastes have attracted lots of interest as an inexpensive source of raw materials due to the rapid increasing of petroleum price.¹ High density polyethylene (HDPE) and polyethylene terephthalate (PET) constitute the major amounts of plastic waste since their annual rates of consumption especially in packaging industry keep increasing.^{2,3} Polymer blending is known as a convenient path to obtain new polymeric materials by combining the excellent properties of two or more polymers.⁴ HDPE/PET blends exhibit intermediate properties of both plastic components which are less brittle than neat PET and stiffer than HDPE.⁵ Jarukumjorn and Char-eunkvun reported that the tensile modulus of recycled HDPE (rHDPE)/recycled PET (rPET) (25/75 and 75/25 wt %) blend which made by melt-mixing in a twin screw extruder were 69 and 23% higher than rHDPE. The rHDPE rich blend displayed better impact performance relative to rPET, which was about threefold increase.⁶ Lei and Wu⁷ produced an *in situ* microfibrillar recycled HDPE/PET (75/25 wt/wt) composites through reactive extrusion and stretching exhibiting an increase in

elongation at break from 7 to 60 kJ/m² when 5 wt % ethylene-glycidyl methacrylate (E-GMA) was introduced

Nowadays, the introduction of nanosize particles such as nanoclay as a reinforcing filler in polymer matrix, can produce nanocomposites that own superior properties when compared to the pure polymer or the conventional composites with micron-sized particles.⁴ Its superior properties including increase in mechanical, thermal, optical clarity and barrier properties, flammability resistance, and high heat deflection temperature, gas barrier performance, dimensional stability, which are of interest and desirable for many applications such as packaging, automotive, aerospace, and civil industries.⁸

The performance of polymer nanoclay composites is dependent upon the aspect ratio (ratio of length to thickness), clay content and state of dispersion of silicate layers.⁸ As established in literature, the degree of dispersion and exfoliation of clay platelets in the polymer matrix are strongly dependence of the clay surface chemistry,^{9,10} molecular weight or properties of the polymer,¹¹ type, and content of compatibilizer^{1,12,13} and another important factor is the processing parameters.^{14–16} Meanwhile, type of morphology and dispersed phase size of blends could be influenced by melt viscosity, composition, interfacial

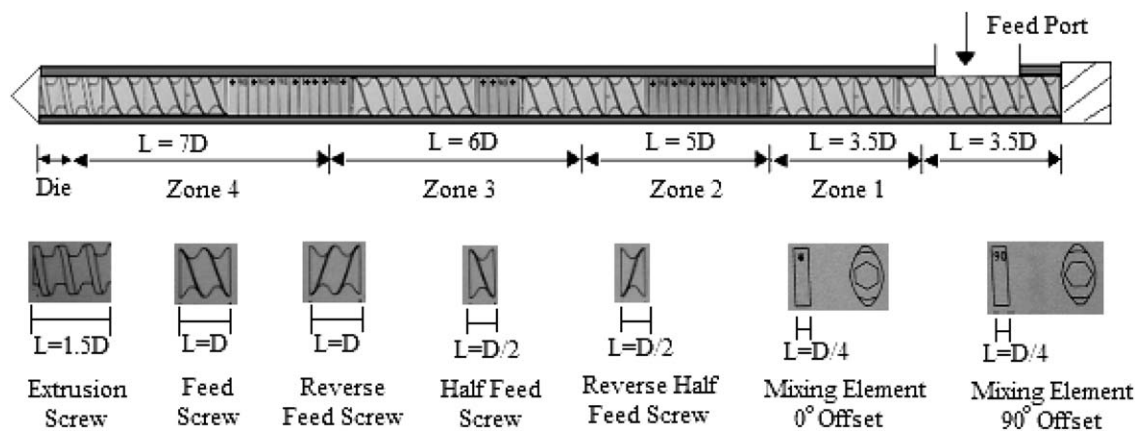


Figure 1. Schematic representation of screw geometry, length expressed in extruder screw diameter.

interactions, and processing conditions.¹⁴ If clay layers are aggregated and remain unseparated, they are named as tactoids. If the polymers diffuse into the interlayer spacing between clay platelets resulting in a well ordered alternating layered silicates and polymer chains by separation less than 20–30 Å, the clays are called intercalated structure. If the individual clay layers are dispersed in the polymer by more than 80 Å, exfoliation is obtained. In order to achieve the best nanocomposite performance, a material with exfoliated clay platelets that distributed homogeneously in the matrix is often required.⁹

The naturally hydrophilic clays have poor miscibility with polymers that are mostly hydrophobic, which resulted in the difficulty of exfoliating clay layers into a polymer matrix. Generally, clays are modified by ion-exchange reactions with cationic surfactants, including primary, secondary, tertiary, and quaternary alkylammonium cations to render its surface more hydrophobic. The existence of alkyl chains intercalated in the interlayer expands the basal spacing between silicate layers, which facilitating exfoliation.¹³ Besides, the incorporation of compatibilizers containing polar functional groups, such as maleic anhydride polyethylene (MAPE) tends to improve the compatibility of PE with clay.¹

Numerous studies have been published on polymer–clay nanocomposites based on single polymer matrix.^{1,9,12,17} Nanocomposites based on blends of two or more polymeric materials are new approach in the nanocomposites studies. In this direction, some studies related to nanocomposites of the blends have been reported, for example, polypropylene (PP)/PET/clay blends,¹⁸ PET waste/poly(methyl methacrylate)/clay blends,¹⁹ polybutylene terephthalate/PE/clay blends.²⁰ However, only a few papers have studied nanoclay composites based on a recycled polymer blend. In this study, the aim was to analyze the effect of polymer/clay compatibility, compounding method, processing parameters and clay loading on the mechanical properties, state of dispersion, and morphological behavior of recycled HDPE/PET/Cloisite 10A (clay) nanocomposites.

EXPERIMENTAL

Raw Materials

Recycled high-density polyethylene (rHDPE, density, 923 kg/m³; melt flow index of 0.72 g/10 min at 190°C, 2.16 kg load) and

recycled PET (rPET, T_g , 74.1°C; cold crystallization peak temperature, 119.9°C; melting peak temperature, 252.5°C and intrinsic viscosity of 0.68 dL/g) from a local plastic recycling plant were used as received. Montmorillonite modified with a dimethyl, benzyl, hydrogenated tallow, quaternary ammonium (CEC = 125 meq/100 g clay, d_{001} = 19.2 Å) was obtained from Southern Clay Products, with trade name of Cloisite 10A (C10A). To improve the compatibility between thermoplastic blends and C10A, two different compatibilizers were used: (1) E-GMA (Lotader AX8840) with 5 g/10 min (190°C, 2.16 kg) of melt index and 8% of glycidyl methacrylate content, and (2) MAPE (melting peak temperature, 135.2°C) with melt index 5 g/10 min (190°C, 2.16 kg) and 1 wt % maleic anhydride content. All the recycled plastics and compatibilizers were supplied by a local factory namely BioComposites Extrusion Sdn. Bhd.

Composites Preparation

Prior to compounding, recycled PET pellets and organoclay, C10A were dried at 100°C for 24 h. Melt mixing of the composite samples was performed in a laboratory scale co-rotating twin screw extruder (model Thermo Prism TSE 16 PC, D = 16 mm, L/D = 25). The detailed screw configuration of this screw is shown in Figure 1. The rHDPE/rPET/C10A [with and without compatibilizer(s)] nanocomposites were prepared using either a one-step or a two-step compounding. The weight ratio of rHDPE/rPET was fixed at 75/25 (wt/wt) which acts as recycled polymer blend matrix. The compatibilizer loading level of E-GMA and MAPE was fixed at 5 and 3% based on the total weight of composites, respectively. The formulated raw materials were first tumble-mixed in sealed plastic bag before melt-blended through extrusion. In the one-step method, all of the raw materials were added simultaneously and compounded at a screw rotating speed of 30 rpm and a barrel temperature profile of 190–240–270–250°C (from feeding to die zones). Meanwhile, in the two-step blending method, a masterbatch was first made by melt-blending both of recycled polymer matrix components (rHDPE and rPET) with the E-GMA in the same weight ratio as in one-step compounding method (75/25/5). In first extrusion, the temperature profile of 190–240–270–250°C with 30 rpm was used. In the second step of extrusion, the masterbatch was blended with C10A (with or without MAPE) at a screw speed of 30 rpm and a temperature profile 170–215–210–

195°C. During the whole extrusion processing, the throughput was set at 1 kg/h and maintained volumetrically.

After extrusion, the extrudates were cooled and granulated into pellets by a crusher. The fine granules were put in to mould with a dimension of $14 \times 14 \times 3 \text{ mm}^3$ and then compression-molded by hot and cold press process (LP50, LABTECH Engineering Company) to make the specimen panels for testing. The compression was performed at processing temperature of 200°C under a pressure of 1000 psi during 15 min (3 min for preheating, 2 min for venting, 5 min for full hot pressing, and 5 min for cold pressing). The area of compression tool is $21 \times 21 \text{ cm}^2$. The specimens were then cut using a table circular-blade saw according to ASTM specifications for mechanical testing.

Four parameters including the absence/presence of compatibilizer(s), compounding method, processing conditions, and clay contents were studied to explore their independent effect.

Changes in the Absence/Presence of Compatibilizer(s). It should be noted that clay content (3 wt %) and preparation method (one-step compounding) are kept constant.

Neat rHDPE/rPET blend, rHDPE/rPET/C10A, rHDPE/rPET/C10A/E-GMA, and rHDPE/rPET/C10A/E-GMA/MAPE nanocomposites with the composition of 75/25, 75/25/3, 75/25/3/5, 75/25/3/5/3 wt % were prepared.

Changes in the Compounding Method. It should be noted that the composition of nanocomposite (3 wt % C10A, 5 wt % E-GMA) is kept constant. Both the (one-step and two-step) compounding procedures and conditions were followed as stated above.

Changes in the Extruder Parameters. It should be noted that the composition of nanocomposite (3 wt % C10A, 5 wt % E-GMA) and preparation method (two-step blending) are kept constant.

Second extrusion temperature profile: 190–240–270–250°C, a higher temperature profile (HTP) was used instead of lower temperature profile (LTP) of 170–215–210–195°C.

Screw rotation speed: Four different speeds, 60, 90, 120, and 150 rpm, were used.

Changes in the Clay Loadings. It should be noted that the compatibilizers (5 wt % E-GMA and 3 wt % MAPE) used in nanocomposite, preparation method (two-step blending), and processing conditions (LTP and 30 rpm) are kept constant. Four different organoclay C10A concentrations, 1, 5, 7, and 9 wt %, were used besides 3 wt %.

Determination of Tensile and Impact Properties

Tensile test was carried out at room temperature in a universal testing machine (model Testometric M350-10CT) at a crosshead speed of 5 mm/min in according with ASTM D638-03 (type I) standard recommendations. Izod impact test was performed at room temperature in a Ray-Ran Universal Pendulum Impact System at velocity of 3.46 ms^{-1} , load weight of 0.452 kg and calibration energy of 2.765 J by following ASTM D 256-05 (Impact) standard recommendations. At least five replicates of

the specimens were tested for each formulation, and the average values were reported.

Dispersion State of Clay in Recycled Polymer Matrix

Wide angle X-ray diffraction (XRD) study was carried out to determine state of intercalation or exfoliation of clay within the polymer matrix. XRD analysis conducted with a D8 Advance diffractometer with $\text{CuK}\alpha$ radiation ($\lambda = 0.154056 \text{ nm}$). The generator was operated at 40 kV and 30 mA. Samples were scanned from $2\theta = 2.3^\circ$ to 12° at a scanning rate of $2^\circ/\text{min}$.

Distribution of Clay and Morphological Behavior

The scanning electron microscopy (SEM) experiment was performed in a VPSEM Philips XL-30 at an accelerating voltage of 15 kV to examine the shape and size of clay as well as the dispersion of clay within the polymer blends on the microscopic scale. The broken surfaces of the tensile test specimens were being sputter-coated with gold before the morphologies of specimens were observed.

RESULTS AND DISCUSSION

Effect of Compatibility Between rHDPE, rPET, and Clay

Table I shows the influence of clay and compatibilizer incorporation on mechanical properties of rHDPE/rPET and rHDPE/rPET/C10A composites. The tensile strength, Young's modulus, elongation at break, and impact strength of nanocomposites have the same trend. The uncompatibilized rHDPE/rPET blend exhibited the reduced mechanical properties when C10A was incorporated, which can be attributed to the bad dispersion of clay within polymer matrix as well as the clay-polymer incompatibility. The previous studies have been reported that clays have a compatibilization effect on the immiscible polymer blend via melt blending.^{19,20} However, in this study, the exclusion use of clay in the recycled HDPE/PET blend without any compatibilizer was not sufficient to compatibilize both of the polymer phases, which agreed with findings reported by Calcagno *et al.*⁴ The incorporation of compatibilizing agents, MAPE and E-GMA in this study, were aided in improving the compatibility of rHDPE, rPET and clay since they are inherently incompatible because of the great difference in polarity (solubility parameters) between them. It is evident from Table I that the presence of compatibilizer in nanocomposites slightly increased the tensile strength and Young's modulus but large enhancement in elongation at break and impact strength were found with respect to the neat rHDPE/rPET and rHDPE/rPET/C10A composite. It is important to note that the tensile strength of composites incorporated with nanoclay is dependent upon several factors such as clay dispersion in the inner and outer layers, interaction between polymer and clay as well as compatibility between polar and non-polar components in the polymer blend.²¹ In the polymer blends, high strain properties such as elongation at break and impact strength are very sensitive to the interphase interactions between the polymer components. The significant enhancement of elongation at break and impact strength indicated the increase of blend ductility and toughness which was because of the improved adhesion between rHDPE-rPET phases by the simultaneous presence of clay and compatibilizer.⁴ By comparing the effectiveness of compatibilizer, the nanocomposite sample incorporated with E-GMA alone

Table I. Effect of Different Compatibilizer on Mechanical Properties of rHDPE/rPET/C10A Nanocomposites Prepared by One-Step Compounding

Material sample	Tensile strength (MPa)	Young's modulus (MPa)	Elongation at break (%)	Impact strength (kJ/m ²)
rHDPE/rPET	15.2 ± 0.3	750 ± 37	7.2 ± 0.4	2.14 ± 0.07
rHDPE/rPET/C10A	13.3 ± 0.1	656 ± 17	6.2 ± 0.4	2.04 ± 0.24
rHDPE/rPET/C10A/MAPE	15.3 ± 0.3	752 ± 26	8.3 ± 0.6	2.26 ± 0.08
rHDPE/rPET/C10A/E-GMA	16.3 ± 0.2	759 ± 75	10.3 ± 0.8	3.04 ± 0.33
rHDPE/rPET/C10A/MAPE/E-GMA	16.0 ± 0.3	756 ± 9	9.1 ± 0.3	3.02 ± 0.21

attained the optimum improvement in the mechanical properties compared to MAPE alone and hybrid compatibilizer system. The tensile strength, Young's modulus, elongation at break, and impact strength for this system were about 22.6, 15.7, 66.6, and 49.0% higher than rHDPE/rPET/C10A nanocomposite containing no compatibilizer. This might be due to the higher reactivity of epoxy functionality in GMA which can react with both hydroxyl and carbonyl end groups of PET than MA that reacts only with hydroxyl ends.²² The obtained results suggest that the existence of hybrid compatibilizer (MAPE /E-GMA) in nanocomposite exceeds the certain saturation compatibilizer level and thus, resulting the lower mechanical properties than E-GMA alone.

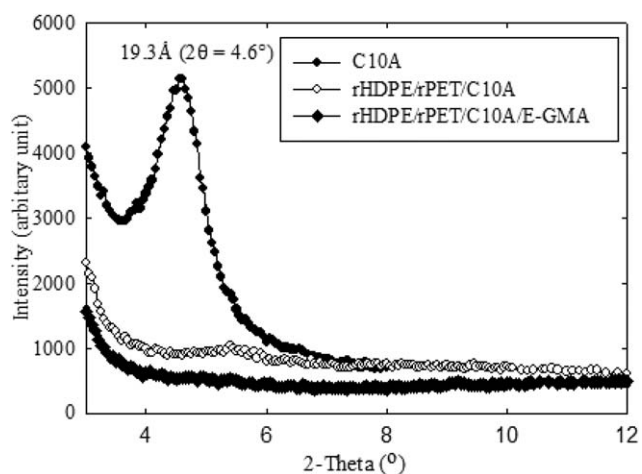
The XRD patterns of the C10A organoclay, uncompatibilized, and compatibilized rHDPE/rPET/C10A nanocomposites are shown in Figure 2. The C10A itself exhibited the characteristic peak at a 2θ of 4.6° corresponding the d-spacing of 19.3Å. This clay peak was not seen clearly in the rHDPE/rPET/C10A nanocomposites with or without compatibilizer, suggesting the intercalation/exfoliation of the C10A clay layers in rHDPE/rPET matrix. As referring to Calcagno *et al.*⁴ who investigated PP/PET blends containing C10A clay and MAPE, the XRD results showed a shift of clay peak from 4.6° to 2.55° with the broadening of the peaks in the nanocomposites that indicated the intercalated structure. Therefore, it is possible to believe that the nanocomposites in this case were more probably found in intercalated structure than exfoliated structure. In the presence of E-GMA, the XRD pattern of nanocomposite exhibited the similar behavior compared to that of the nanocomposites without E-GMA, somehow, its intensity was slightly lowered for the system containing E-GMA. This indicates a little enhancement in the degree of exfoliation (dispersion) of layered silicates in the compatibilized nanocomposite.

Figure 3 presents SEM images for the uncompatibilized and compatibilized rHDPE/rPET/C10A nanocomposites with MAPE or/and E-GMA. As observed in the Figure 3(a), the uncompatibilized samples exhibited the globular morphology where the rPET phase dispersed as spherical domains with inconsistent size in rHDPE matrix. The rHDPE and rPET phases were unbounded to each other which indicating the weak interfacial adhesion between both polymer components. This could be due to the immiscible nature of the HDPE and PET.³ This is the reason why the uncompatibilized blend showed the reduced mechanical properties when C10A clay was incorporated, as shown in Table I. In the Figure 3(b), it is evident that the

presence of MAPE in rHDPE/rPET/C10A tends to promote a little adherence between both polymer phases. Somehow, SEM image of the MAPE compatibilized nanocomposite still presents a two phase structure. In comparison, Figure 3(c,d) shows that the morphology of the samples with the presence of E-GMA compatibilizer was significantly changed from coarse and obvious phase segregation structure to finer and homogenous structure. According to Chen *et al.*,⁵ E-GMA is the most effective compatibilizer to enhance the compatibility of hydrophobic HDPE and hydrophilic PET by reducing the interfacial tension and particle size distribution of rPET within the rHDPE matrix. This is due to the higher reactivity of epoxy functionality of GMA than anhydride functionality of MA.³ However, when MAPE is presented with E-GMA in the samples, the blend compatibility was not good as the samples with E-GMA alone. This indicates the incorporation of E-GMA was sufficient to promote a good interaction between the rHDPE and rPET with C10A clay, as proven in the optimum increment of tensile and impact properties in Table I. The SEM image from Figure 3(d) depicts that the excess compatibilizer contributed to a negative effect on the blend homogeneity and structure fineness and so to the reduction in mechanical performance properties.

Effect of Compounding Method

The effect of preparation method for rHDPE/rPET/C10A nanocomposites containing E-GMA compatibilizer alone is shown in Table II. The tensile and impact properties of the

**Figure 2.** XRD patterns of the C10A and rHDPE/rPET/C10A nanocomposites with and without compatibilizer.

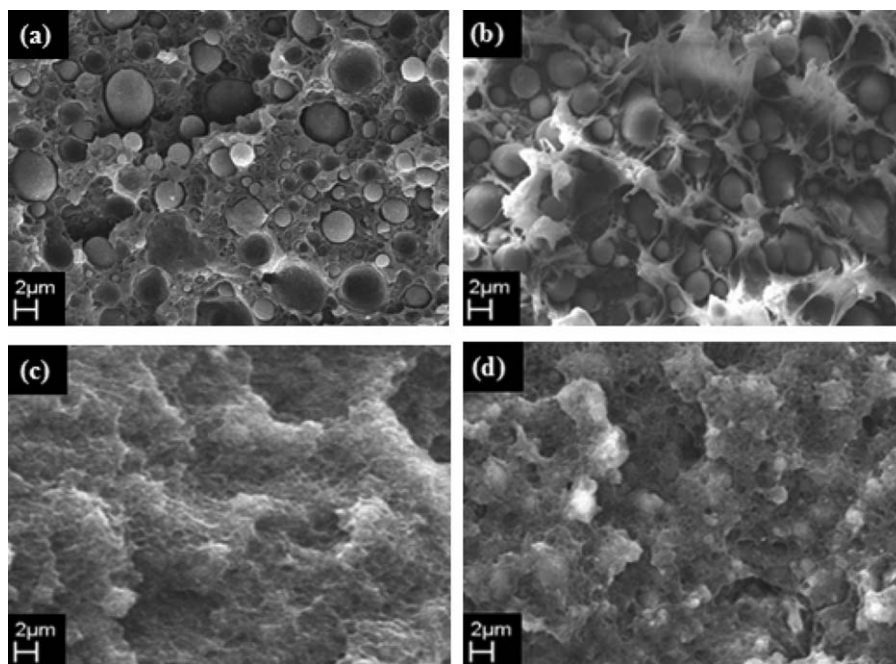


Figure 3. SEM images of rHDPE/rPET/C10A (a) without compatibilizer, (b) with MAPE, (c) with E-GMA, (d) with MAPE and E-GMA at magnification of $\times 1000$.

Table II. Effect of Compounding Method on Mechanical Properties of Organoclay Nanocomposites

Preparation method	Tensile strength (MPa)	Young's modulus (MPa)	Elongation at break (%)	Impact strength (kJ/m ²)
One-step	16.0 \pm 0.3	756 \pm 9	9.1 \pm 0.3	3.02 \pm 0.21
Two-step	17.3 \pm 0.1	855 \pm 19	15.1 \pm 0.8	3.74 \pm 0.55

nanocomposite prepared using the two-step compounding method was higher than those compounded in one-step compounding. The improvements in tensile strength, Young's modulus, elongation at break, and impact strength were about 8.1%, 13.1%, 64.7%, and 23.8%, respectively. This could be explained in Figure 4 that depicts the typical tensile fracture surfaces of nanocomposites containing 3 wt % C10A processed with one-step compounding and two-step compounding. As observed in the figure, the sample made with two-step compounding presented such thorn like fracture structures of rHDPE matrix that

believed to be of typical brittle behavior.⁵ This is in agreement with the remarkable improvement results obtained from elongation at break and impact strength (Table II). The XRD pattern results in Figure 5 describes a shift of clay peak from 4.6° to 2.67° in the nanocomposites that indicated the intercalated structure; but, the compounding method (one-step and two-step) on preparing C10A nanocomposites made no changes with the clay peak position. This means that the degree of intercalation is independent of the compounding method, in the range investigated. Somehow, the intensity of the shifted clay

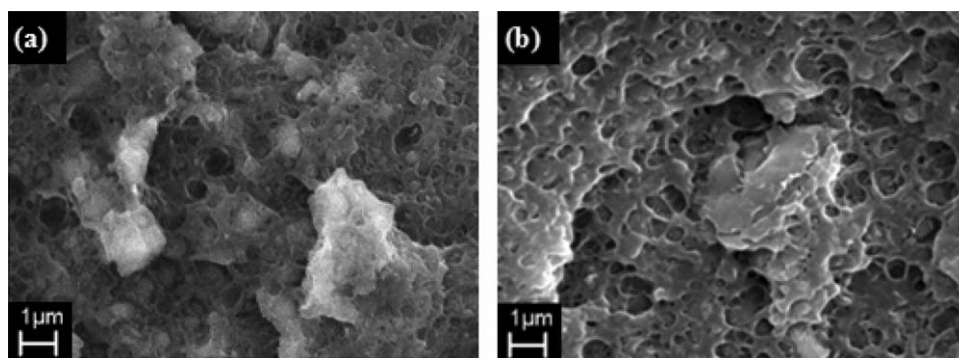


Figure 4. Tensile fracture surface of rHDPE/rPET/C10A sample containing compatibilizers made with (a) one-step compounding and (b) two-step compounding at magnification of $\times 3000$.

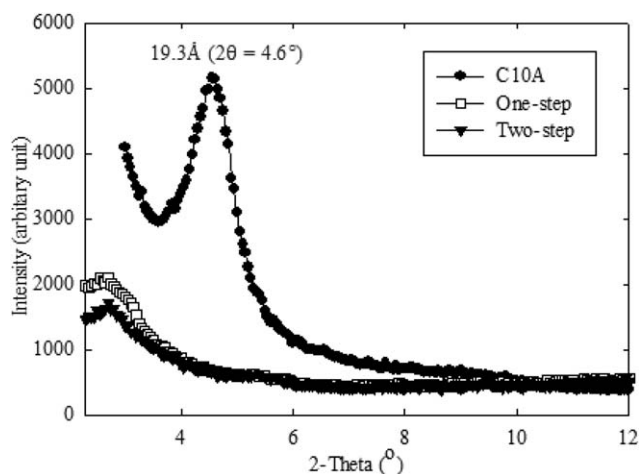


Figure 5. XRD patterns of the C10A and its nanocomposites prepared by one-step and two-step compounding method.

peak was slightly lowered for the nanocomposites prepared by two-step method. This indicates the compounding method of nanocomposites had a certain effect on the degree of exfoliation. From these results, two-step compounding method appeared to be the best approach of incorporating organoclay in recycled polymer blends.

Effect of Extrusion Parameters

The effect of extruder parameters on the mechanical, and morphology behavior of rHDPE/rPET/C10A nanocomposites with 5% E-GMA was studied by changing extrusion temperature profile and screw rotation speed in the extruder, independently. Table III describes the effect of extrusion parameters on the mechanical properties of 3 wt % C10A nanocomposites prepared by two-step compounding method. As it can be seen in this table, the nanocomposites that extruded at HTP exhibited slightly higher mechanical properties compared to those extruded at LTP. This can be confirmed by the XRD results in Figure 6. It can be observed that the peak position of nanocomposites do not change with extrusion temperature profile, which indicating the degree of intercalation is independent of the extrusion temperature, in the range investigated. As the interlayer spacing of both nanocomposites (36.5 Å for those extruded at HTP and 32.5 Å for those extruded at LTP) is higher than for native C10A (19.3 Å), it may be concluded that

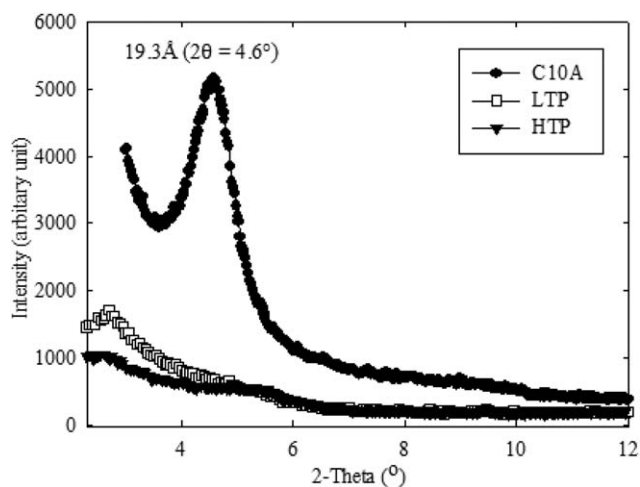


Figure 6. XRD patterns of the C10A and its nanocomposites prepared with LTP and HTP at 30 rpm.

the degradation of quaternary ammonium ions is not occurred during the intercalation process: when the extrusion temperature is higher, diffusion of polymer chains is getting more rapid and thus allows intercalation process before eventual degradation of the quaternary ammonium ions.¹³ Interestingly, in state of intensity, nanocomposite obtained at HTP is lower compared to LTP. This means that a higher extrusion temperature leads to a higher degree of exfoliation and so to an increase in general mechanical properties (Table III). This could be due to the improved degree of delamination as a consequence of the rapid diffusion of the polymer chains into the clay galleries generated when the extrusion temperature increased.

Referring to Table III again, the tensile strength and Young's modulus of nanocomposites increased with increasing the screw speed from 30 to 90 rpm and then decreased with further increasing screw speed from 90 to 150 rpm. In general, the screw rotation speed is correlated to the shear stress applied and residence time of composite material during mixing in extruder. The increase of screw speed up to a certain level will apply higher shear on the melt and thus promotes better dispersion of nanoclay within the polymer blend which resulting in improved mechanical properties.¹⁴ Somehow, at the same, the residence time of melt will decrease with increasing screw speed. As reported in Zhang *et al.*,¹⁶ the technical importance of

Table III. Effect of Extrusion Parameters on Mechanical Properties of Nanocomposites

Extrusion temperature (°C)	Screw rotation speed (rpm)	Tensile strength (MPa)	Young's modulus (MPa)	Elongation at break (%)	Impact strength (kJ/m ²)
HTP	30	16.2 ± 0.1	833 ± 40	14.3 ± 0.1	3.35 ± 0.15
LTP	30	16.0 ± 0.2	818 ± 42	16.0 ± 0.6	2.96 ± 0.06
LTP	60	16.2 ± 0.5	826 ± 50	15.3 ± 0.1	2.82 ± 0.17
LTP	90	16.5 ± 0.3	1007 ± 43	12.1 ± 0.9	2.41 ± 0.07
LTP	120	16.2 ± 0.1	850 ± 42	11.6 ± 0.1	2.37 ± 0.06
LTP	150	15.4 ± 0.4	786 ± 70	9.1 ± 0.8	2.19 ± 0.03

Note: HTP is at 190–240–270–250°C; LTP is at 170–215–210–195°C. Screw torque value is 12 Nm.

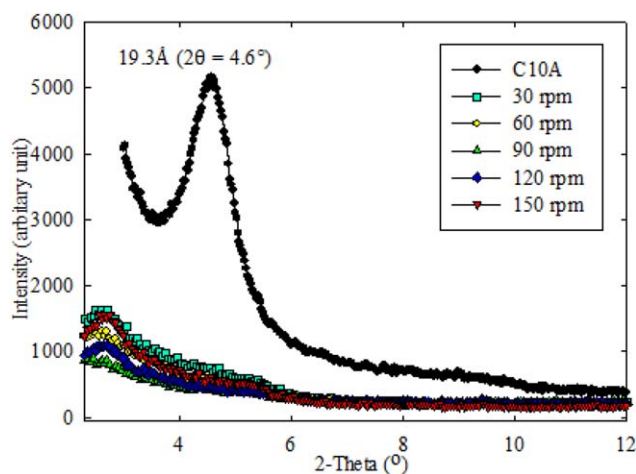


Figure 7. XRD patterns of the C10A and its nanocomposites prepared with various screw rotation speeds at LTP. [Color figure can be viewed in the online issue, which is available at wileyonlinelibrary.com.]

reaction to manufacture composites requires high shear stress at polymer melt state and suitable residence time. In this study, screw speed of 90 rpm leads to optimum tensile strength (16.5 MPa) and Young's modulus (1007 MPa) compared to 30, 60, 120, and 150 rpm. This is attributed to higher shear rate obtained at 90 rpm screw speed than 30 and 60 rpm. Also, 90 rpm obtained higher residence time than the screw speed of 120 and 150 rpm. On the other hand, the elongation at break and impact resistance decreased with the increasing screw speed. The reduced elongation at break and impact resistance can be associated with the loss in the ductility index due to the increased of the stiffness value for the nanocomposite prepared with the screw speed from 30 to 90 rpm.

Figure 7 shows the XRD pattern results of organoclay C10A and its nanocomposites prepared with various screw rotation speeds (30, 60, 90, 120, and 150 rpm) at LTP. The interlayer spacing of C10A increased from 19.3 Å (4.6°) to about 33 Å (2.68°) in the nanocomposites by the intercalation of the polymer inside the clay galleries. Somehow, as in the case of the processing temperature profile, no significant differences in the peak position among the nanocomposites prepared with different screw speeds were observed which shows the same degree of intercalation obtained as explained above. However, the screw speed has a great influence on the state of exfoliation by showing the changes in the intensity. A lower intensity of XRD pattern

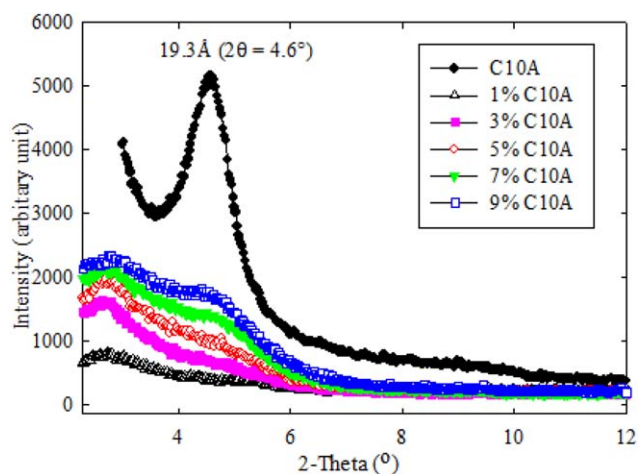


Figure 8. XRD patterns of the C10A and its nanocomposites with respect to organoclay C10A loadings. [Color figure can be viewed in the online issue, which is available at wileyonlinelibrary.com.]

indicates a higher degree of exfoliation. Once more, higher screw speed generated a higher shear rate, which resulted in a higher degree of clay dispersion within polymer matrix. Exceeding the optimum screw speed, 90 rpm in this study, further increasing of screw speed will generate insufficient residence times of the melt in the extruder for the complete compounding, which led to the incomplete intercalation or exfoliation behavior of clay in the polymer matrix. This result is supported by the tensile strength and modulus as shown in Table III.

Effect of Clay Loadings

The mechanical properties of nanocomposites with 3 wt % C10A are presented in Table IV. In this case, the rHDPE/rPET blend compatibilized with 5 wt % E-GMA without organoclay is acting as a control sample. The introduction of organoclay from 1 to 9 wt % into the rHDPE/rPET blend matrix decreased the tensile strength gradually by 7.9–23.6% compared to the control sample (19.1 MPa). As reported in previous finding on PP/PET blend localized by nanoclay, the reduction of tensile strength could be explained by the brittle mechanical behavior of PET-rich blend that indicates the inter-connection of the stress concentration on the platelet tactoids of the nanoparticles in a network like structure, which capable to form crazes and so their ability to grow in the PET matrix phase.¹⁸ Somehow, the Young's modulus improved for the composites with the increase of nanoclay content up to 9 wt %, which was about

Table IV. Effect of Clay Content on Mechanical Properties of Nanocomposites

Clay content (wt %)	Tensile strength (MPa)	Young's modulus (MPa)	Elongation at break (%)	Impact strength (kJ/m ²)
0	19.1 ± 0.4	821 ± 15	10.6 ± 0.6	7.31 ± 0.19
1	17.6 ± 0.2	832 ± 44	15.0 ± 0.6	4.43 ± 0.13
3	17.3 ± 0.1	855 ± 19	14.7 ± 1.0	3.74 ± 0.55
5	16.5 ± 0.3	879 ± 11	12.2 ± 1.3	2.67 ± 0.14
7	16.3 ± 0.2	926 ± 51	12.0 ± 1.0	2.33 ± 0.58
9	14.6 ± 0.2	978 ± 69	7.9 ± 0.7	2.26 ± 0.14

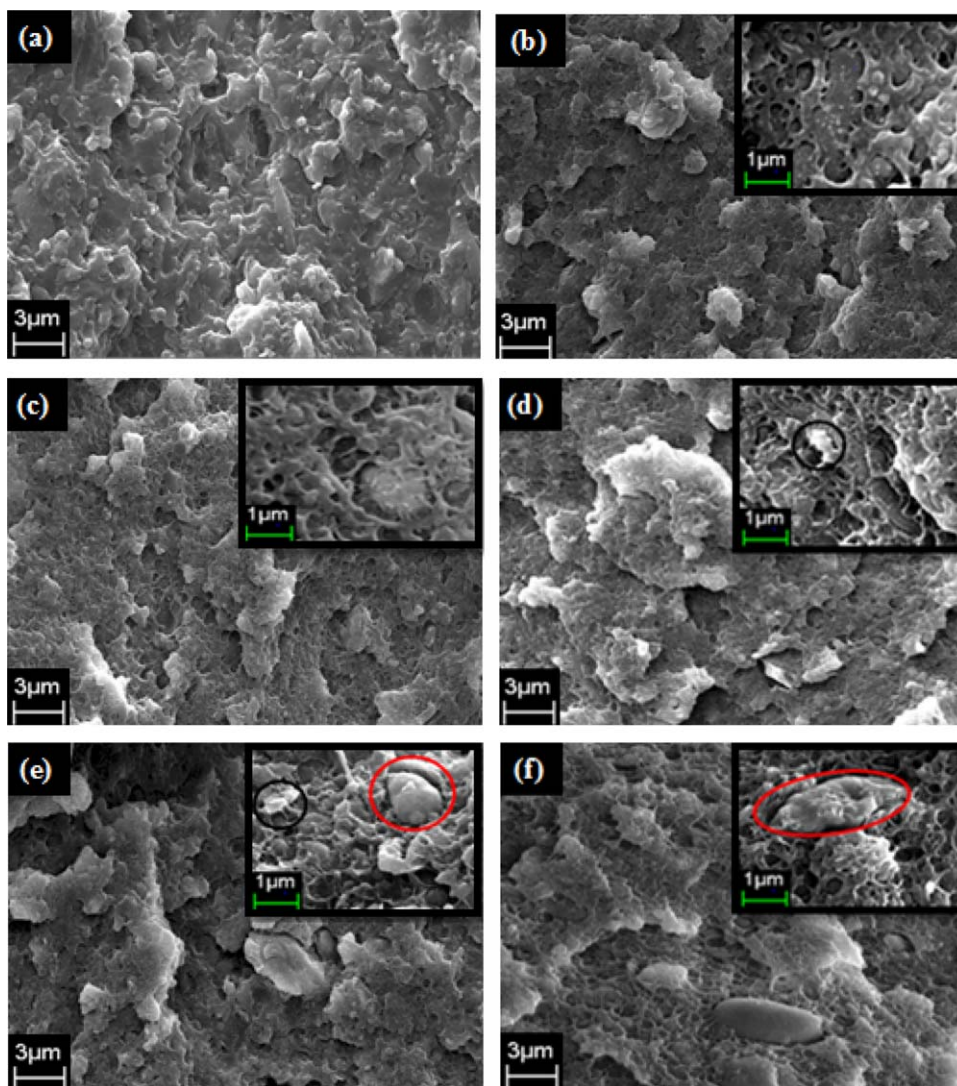


Figure 9. Tensile fracture surface of rHDPE/rPET blend and rHDPE/rPET/C10A nanocomposite sample with respect to organoclay C10A loadings: (a) 0 wt %, (b) 1 wt %, (c) 3 wt %, (d) 5 wt %, (e) 7 wt %, and (f) 9 wt %. [Color figure can be viewed in the online issue, which is available at wileyonlinelibrary.com.]

156 MPa (19%) higher than control sample. The improvement of modulus in nanocomposites is due to the constrained mobility of polymer chains in the presence of the nanoclay particles in polymer matrix.¹² The elongation at break was higher when a small amount of clay, 1–7 wt % C10A in this study, was used. The nanocomposite with 1 wt % C10A exhibited the highest value of elongation at break which increased about 40.9% compared with control sample, indicating an increase in toughness.⁴ However, further increasing the clay content, elongation at break values started to drop gradually. This is because the increment of clay content will inhibit the plastic deformation of polymer matrix and make the nanocomposite become difficult to elongate.²³ Similarly, the impact strength decreased as clay content increased in nanocomposite samples. Unlike elongation at break result, all nanocomposite samples exhibited lower impact strength compared to control sample. The downward trends in elongation at break and impact strength are in agreement with the increasing stiffness.²³

Figure 8 shows the XRD patterns of the C10A and its nanocomposites with respect to clay loadings. As stated earlier, the characteristic peak of clay itself before compounding is situated at 2θ of 4.6° with the interlayer spacing of 19.3 \AA . The shifting of the clay peak position to lower angles region (2.69°) in 1 wt % C10A nanocomposites indicated the diffusion of rHDPE/rPET chains inside the clay galleries with a d-spacing of 32.9 \AA . The small and broad peak with very low intensity in nanocomposite with 1 wt % C10A suggests a partially exfoliated structure. By increasing the clay loading in rHDPE/rPET blend from 1 to 3, 5, 7, and 9 wt %, XRD peak was slightly shifted toward the higher angles at 2.71 , 2.73 , 2.74 , and 2.79° , respectively, and at the same time the d-spacing and intensity was increased accordingly. This can be associated with the difference in the state of clay dispersion which affected by the presence of clay agglomerates with the increasing clay loading. Moreover, the presence of other peaks at higher angles (4.63° and 4.83°) in nanocomposites with 7 and 9 wt % C10A seems to present a parallel

stacking of the silicate layers which is agreed by Kerboua *et al.*¹⁹ Therefore, it is reasonable to conclude that with higher clay content above 7 wt % C10A in blend, silicate layers are intercalated and stacked.

Figure 9 illustrates the tensile fracture surface morphologies of rHDPE/rPET blend and rHDPE/rPET/C10A nanocomposite sample with different clay loadings. Based on Figure 9(a), the polymer blend matrix displayed single phase structure morphology of an obvious homogenous mixing between rHDPE and rPET components with the aids of E-GMA compatibilizer, as stated in our previous study.³ The fracture surface of matrix presents the typical behavior of a brittle material, and by incorporating clay inside the polymer matrix this behavior is not markedly changed. However, it is interesting to observe that the clay played a crucial role in reducing the particle sizes of rHDPE/rPET blends. This can be ascribed to the increase of the matrix phase's viscosity with the presence of clay.²⁴ For low clay contents up to 3 wt %, no visible of the clay aggregates in Figure 9(b,c) which suggesting a fine dispersion of clay in the rHDPE/rPET matrix. For higher clay contents at 5, 7 and 9 wt %, as can be seen in Figure 9(d-f), some clay aggregates [black circles in high magnification images of Figure 9 (d,e)] were found. Besides, more big agglomerates with irregular shape are seen as in red circles from the high magnification images in Figure 9 (e,f). These observations give evidence of some clay C10A encapsulation by E-GMA or MAPE compatibilizer. This result is in agreement with the results of tensile and impact properties in Table IV.

CONCLUSIONS

Recycled HDPE/PET/clay nanocomposites have been prepared via melt intercalation and their mechanical properties, clay dispersion and morphology behavior were investigated. Analyzing the compatibility between rHDPE, rPET and C10A (by using different compatibilizers), it was demonstrated that the highest effect in improving mechanical properties and blend miscibility were obtained for the simultaneous addition of C10A and E-GMA into recycled HDPE/PET blend. Two-step compounding method was better approach than one-step compounding for incorporating C10A in recycled HDPE/PET blend which was first extruded as matrix. The degree of intercalation which interpreted by interlayer spacing is obviously unaffected by the parameters. However, increasing mixing temperature and shear stress with suitable residence time in extruder induce rapid diffusion of polymer chains and thus improve the exfoliation of clays. Higher extrusion temperature profile (HTP) and screw rotation speed of 90 rpm led to the optimum enhancement of overall mechanical properties and dispersion level from the XRD pattern showed. Young's modulus of nanocomposite increases with increasing organoclay loading. Tensile strength slightly drops while impact strength dramatically decreases with the clay fraction, which conform the increase of stiffness. Although the clay addition at low content causes a higher elongation at break of composites, this effect is gradually decreased as a function of clay, which is a sign of a worsen clay dispersion, as exhibited by the clay agglomerates in SEM images.

ACKNOWLEDGMENTS

The authors gratefully acknowledge the National University of Malaysia, UKM Research Grant DPP-2014-034, BioComposites Extrusion Sdn Bhd, and the Ministry of Higher Education Malaysia MyPHD Scholarship Programme for the donation of materials and financial support.

REFERENCES

1. Lei, Y.; Wu, Q.; Clemons, C. M. *J. Appl. Polym. Sci.* **2007**, *103*, 3056.
2. Chen, R. S.; Ab Ghani, M. H.; Salleh, M. N.; Ahmad, S.; Tarawneh, M. A. *J. Appl. Polym. Sci.* **2015**, 132.
3. Chen, R. S.; Ab Ghani, M. H.; Salleh, M. N.; Ahmad, S.; Gan, S. *Mater. Sci. Appl.* **2014**, 5.
4. Calcagno, C. I. W.; Mariani, C. M.; Teixeira, S. R.; Mauler, R. S. *Compos. Sci. Technol.* **2008**, *68*, 2193.
5. Chen, R. S.; Ab Ghani, M. H.; Ahmad, S.; Salleh, M. N.; Tarawneh, M. A. *J. Compos. Mater.* **2014**, 1.
6. Jarukumjorn, K.; Chareunkvun, S. *Suranaree J. Sci. Technol.* **2007**, *14*, 1.
7. Lei, Y.; Wu, Q.; Zhang, Q. *Compos. Part A* **2009**, *40*, 904.
8. Zainuddin, S.; Hosur, M. V.; Zhou, Y.; Narteh, A. T.; Kumar, A.; Jeelani, S. *Mater. Sci. Eng. A* **2010**, *527*, 7920.
9. Tarapow, J. A.; Bernai, C. R.; Alvarez, V. A. *J. Appl. Polym. Sci.* **2009**, *111*, 768.
10. Santos, K. S.; Liberman, S. A.; Oviedo, M. A. S.; Mauler, R. S. *Compos. Part A: Appl. Sci. Manuf.* **2009**, *40*, 1199.
11. Hotta, S.; Paul, D. R. *Polymer* **2004**, *45*, 7639.
12. Bahrami, S. H.; Mirzaie, Z. *World Appl. Sci. J.* **2011**, *13*, 493.
13. Lertwimolnun, W.; Vergnes, B. *Polymer* **2005**, *46*, 3462.
14. Kord, B.; Ghasemi, I.; Najafi, A.; Kiaefar, A. *World Appl. Sci. J.* **2011**, *13*, 1147.
15. Mohan, T. P.; Kanny, K. *Mater. Sci. Appl.* **2011**, *2*, 785.
16. Zhang, Z.-X.; Gao, C.; Xin, Z. X.; Kim, J. K. *Compos. Part B Eng.* **2012**, *43*, 2047.
17. Zhu, S.; Chen, J.; Li, H.; Cao, Y. *J. Appl. Polym. Sci.* **2013**, *128*, 3876.
18. Entezem, M.; Khonakdar, H. A.; Yousefi, A. A.; Jafari, S. H.; Wagenknecht, U.; Heinrich, G. *Mater. Des.* **2013**, *45*, 110.
19. Kerboua, N.; Cinausero, N.; Sadoun, T.; Lopez-Cuesta, J. M. *J. Appl. Polym. Sci.* **2010**, *117*, 129.
20. Hong, J. S.; Kim, Y. K.; Ahn, K. H.; Lee, S. J.; Kim, C. *Rheol. Acta* **2007**, *46*, 469.
21. David, R.; Tambe, S. P.; Singh, S. K.; Raja, V. S.; Kumar, D. *Surf. Coat. Technol.* **2011**, *205*, 5470.
22. Mbarek, S.; Jaziri, M.; Chalamet, Y.; Carrot, C. *J. Appl. Polym. Sci.* **2010**, *117*, 1683.
23. Salmah, S. A. G. H.; Hazwan, K. *Malaysian Polym. J.* **2008**, *3*, 39.
24. Mallick, S.; Khatua, B. B. *J. Appl. Polym. Sci.* **2011**, *121*, 359.